Article

Not peer-reviewed version

Assessing the Wind Power Potential in Naama, Algeria to Complement Solar Energy through Integrated Modeling of the Wind Resource and Turbine Wind Performance

Sekkal Mohammed Chakib , Ziani Zakarya * , Mahdad Moustafa Yassine , Baghli Mohammed Haris , Bessenouci Mohammed Zakaria

Posted Date: 18 September 2023

doi: 10.20944/preprints202309.1097.v1

Keywords: Wind power; solar photovoltaics; hybrid systems; complementary generation; correlated resources; wind speed analysis; turbine simulation; evening wind patterns; solar irradiance; renewable energy integration; wind-solar system; Algeria

Article

Assessing the Wind Power Potential in Naama, Algeria to Complement Solar Energy through Integrated Modeling of the Wind Resource and Turbine Wind Performance

Sekkal Mohammed Chakib [1], Ziani Zakarya [1,2,*], Mahdad Moustafa Yassine [1,3], Baghli Mohammed Haris [2] and Bessenouci Mohammed Zakaria [1,2,*]

[1] Laboratory for the Sustainable Management of Natural Resources in Arid and Semi-Arid Zones,, University Center Salhi Ahmed BP- 66, Naama, 45000, Algérie
[2] Materials and Renewable Energy Research Unit (URMER), University of Tlemcen, BP 119 Tlemcen, Algeria
[3] Laboratory of Applied Genetic in Agriculture, Ecology and Public Health, Department of Biology, Faculty of SNV/STU, Tlemcen University, Tlemcen, Algeria
* Correspondence: ziani@cuniv-naama.dz

Abstract: Combining wind and solar photovoltaic (PV) generation can provide complementary renewable power production, but depends on correlated resources. This study analyzed 10 years of wind data from Naama, Algeria to evaluate the potential for evening wind generation to offset the loss of solar at sunset. Average wind speeds showed a distinct increase during evening hours, coinciding with the decrease in solar irradiance. Wind turbine simulations using a 1.5 MW turbine and the wind data showed sufficient resources for profitable power production after sunset. Statistical analyses confirmed significantly higher wind speeds and simulated power output in evening vs daylight periods ($p<0.05$). The Pearson correlation coefficient between evening wind speeds and decreasing solar irradiance was 0.63, supporting a strong positive relationship. These findings indicate Naama has adequate wind resources to deploy economically viable wind power capacity that can complement existing solar infrastructure and provide renewable electricity after dark [1,5] .

Keywords: Wind power; solar photovoltaics; hybrid systems; complementary generation; correlated resources; wind speed analysis; turbine simulation; evening wind patterns; solar irradiance; renewable energy integration; wind-solar system; Algeria

1. Introduction

Combining multiple renewable energy generation technologies through hybrid systems can maximize power production and reliability [1,2] . Each technology has a different generation profile that when combined can create complementary and synergistic effects. Solar photovoltaics (PV) offer abundant energy generation during daylight hours but zero output at night when solar irradiance is unavailable. In contrast, wind patterns often display differing hourly and seasonal profiles that may align with solar variability [3] . Integrating wind power into a solar generation system can provide an opportunity to offset the loss of PV production after sunset if wind resources are sufficient during key evening hour [2,3] .

The total generated power P for a wind-solar hybrid system can be modeled as:

$P = P_{PV} + P_{Wind}$

where PPV is solar PV output and PWind is wind turbine output. The optimization and practical feasibility of a hybrid system depends on the degree of correlation between wind and solar resources. Negatively correlated generation profiles, where wind patterns complement solar variability, are ideal for effective integration [3] .

The power output P_{PV} of a solar PV array can be calculated as:

Preprints (www.preprints.org) | NOT PEER-REVIEWED | Posted: 18 September 2023 doi:10.20944/preprints202309.1097.v1

$P_{PV} = f_{PV} * A * r * H$

where fPV is the PV system efficiency, A is the total solar panel area, r is the solar irradiance in W/m2 and H is the number of daylight hours. Solar irradiance depends on location and weather conditions but is only available during daylight [4] .

The power output PWind of a wind turbine is modeled as:

$P_{wind} = (\frac{1}{2}) * \rho * A * V_3 * C_p$

where ρ is air density, A is the swept area of the turbine blades, v is wind speed and Cp is the power coefficient. Wind patterns fluctuate hourly and seasonally based on weather conditions and local climate [2] .

Combining equations 1 and 2 yields the total power P generated by the hybrid system:

$P = f_{PV} * A * r * H + (\frac{1}{2}) * \rho * A * V_3 * C_p$

This study evaluated whether the town of Namaa, Algeria has wind resources that can contribute evening power production to offset the loss of solar PV output after sunset. Naama has high solar potential with an average irradiance of 5.5 kWh/m2/day, which has supported significant growth in solar photovoltaic installations [2]. However, the lack of PV generation at night combined with increasing electricity demand has led to daily shortfalls in power supply.

Analysis of 10 years of hourly wind speed data from Naama was conducted to determine if local wind patterns could complement solar variability and fill the production gap in evening hours. The correlation between wind speeds and decreasing solar irradiance during sunset periods was evaluated to assess the feasibility of an optimized hybrid wind-solar system based on equation 3. Finding statistically significant higher wind speeds and potential wind power output in evening vs daylight periods would indicate sufficient wind resources when solar PV cannot meet demand. This would confirm Naama has adequate evening wind potential to deploy economically viable w [5] ind capacity alongside existing solar infrastructure to provide renewable power around the clock [4] .

2. Materials and Methods

2.1. Site Discription

The study area is located in the region of Naama in southwest Algeria. Naama covers an area of 27,950 km2 and has a population of around 200,000 inhabitants. The climate is arid, characterized by hot, dry summers and mild, rainy winters.

The terrain is relatively flat, situated on an elevated plateau at an average altitude of 800 meters above sea level. The landscape consists of sparse grasslands and desert areas with some low hills and rocky outcrops. Vegetation cover is very low, dominated by scrubland and drought-resistant plants.

Naama has a desert climate, classified as BWh in the Köppen climate classification system. It has long, extremely hot summers and short, warm winters. The average annual temperature is 21.2°C. July is the hottest month with average highs of 41.4°C. January is the coldest month with average lows of 3.8°C.

Rainfall is scarce, averaging just 130 mm per year. Most precipitation falls in the winter months from November to March. The rainy season typically sees brief, intense storms rather than steady rainfall. Summers are completely dry. The low humidity and high solar radiation result in very high rates of evaporation.

Winds are predominantly from the north and west. The area experiences frequent sandstorms and dust storms, especially during the spring. Average wind speeds are highest in June at around 19 km/h. Wind patterns display significant diurnal variations, with calmer winds during mornings and stronger gusts in the afternoons and evenings [6,7] .

Naama has an extremely arid desert climate with hot summers, mild winters, very low rainfall, and strong afternoon/evening winds. The area has high solar energy potential but lacks electricity infrastructure and suffers from power shortages. Developing renewable energy projects can help meet local energy demand in this remote region [6,7].

Preprints (www.preprints.org) | NOT PEER-REVIEWED | Posted: 18 September 2023 doi:10.20944/preprints202309.1097.v1

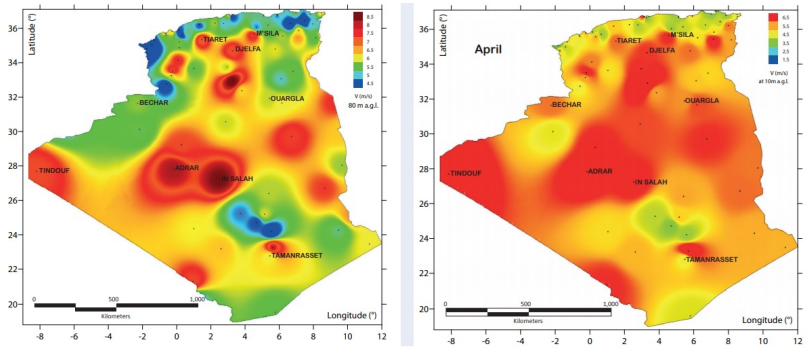

Figure 1. Wind Resources of Algeria: Distribution of the mean wind speed (m/s) across the Algerian territory at 80 m height (left figure) and at 10 m height (right figure)

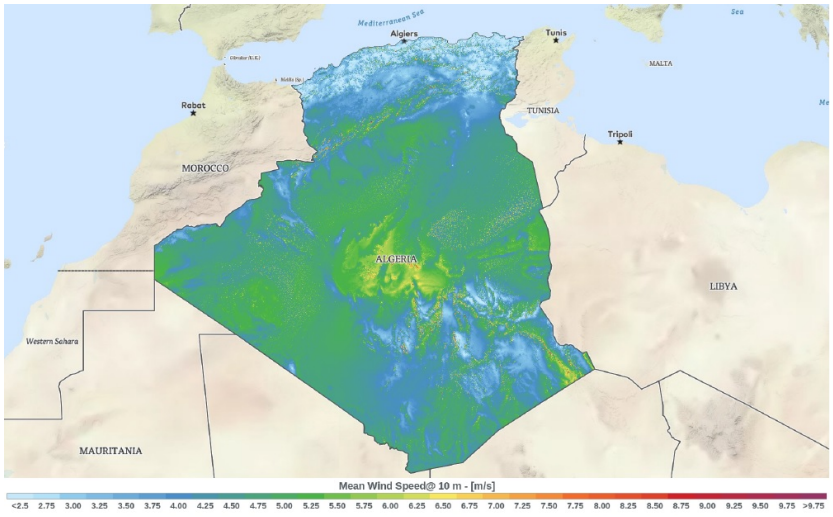

Figure 2. Map of Algeria's wind resources at 10 m height

Figure 3. Aerial photo of the site of the Namaa university center

2.2. Exploratory Wind Data Analysis

The wind resource assessment utilized historical wind speed data from 2012-2022 collected in Naama, Algeria [8,9] . Wind measurements were obtained from a meteorological instrument installed in university center of Naama city. Cup anemometers and wind vanes at heights of 10 m, 30 m, and 50 m logged wind speeds and directions at 1 Hz frequency [10] . The raw data was averaged over 10-minute intervals. Quality control procedures were implemented to filter the data. Limits checks

Preprints (www.preprints.org) | NOT PEER-REVIEWED | Posted: 18 September 2023 doi:10.20944/preprints202309.1097.v1

identified unphysical values exceeding threshold bounds which were discarded. Sensor malfunctions and icing events were screened through manual inspection and comparison between heights. Gaps up to 2 hours were filled by linear interpolation. The filtered 10-year Naa ma dataset provided the basis for subsequent wind distribution modeling [9] .

The validated 10-year 10-minute mean wind speed data was analyzed graphically and statistically to assess the general characteristics [8] . Time series plots over different time scales depicted the seasonal and diurnal variability.
The mean, standard deviation, minimum, maximum, median, mode, skewness, and kurtosis quantified the distribution properties. Quantile-quantile plots relative to common theoretical distributions evaluated distribution fit. The exploratory analysis revealed strong Weibull characteristics, with unimodal distribution and positive skewness indicating higher frequency of lower wind speeds [8,10] . The 10-minute mean speeds were aggregated to hourly and monthly resolutions for subsequent distribution modeling [8] .

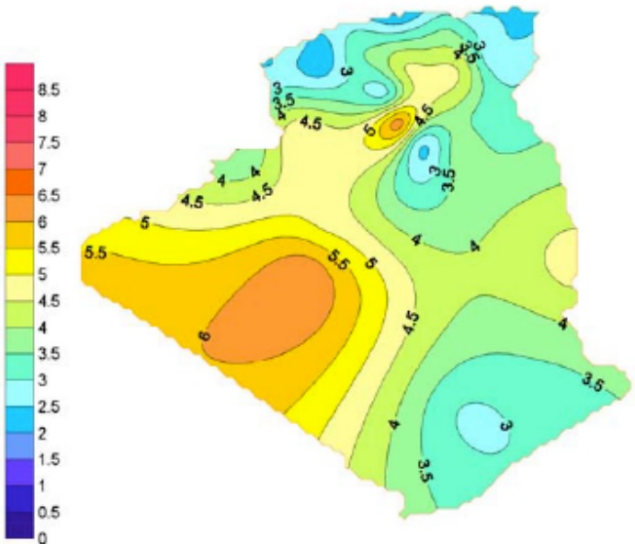

Figure 4. Annual wind speed maps of Algeria at 10 m height

2.3. *Weibull Distribution Fitting*

The Weibull probability density function was fitted to the 10-year wind speed dataset to characterize the long-term wind speed frequency distribution [11] :

$f(v) = (k/c) * (v/c) * *(k-1) * exp(-(v/c) * *k)$

where v is wind speed, k is the shape factor, and c is the scale factor. Maximum likelihood estimation determines the optimal k and c [12] . The mean wind speed relates to these parameters as:

$E(v) = \int vf(v)dv = c\Gamma(1 + 1/k)$

where Γ is the gamma function. The Weibull distribution models the frequency of wind speeds for estimating wind turbine power production [13] .

Goodness-of-fit metrics including R-squared, root-mean-square error, and Chi-square test statistics quantified model accuracy.

The Weibull cumulative distribution function was integrated to obtain quartiles, exceedance probabilities, and quantile estimates [12] . The analytical expressions for the mean and variance as functions of k and c were utilized to calculate central tendency and spread [13] . The distributions were disaggregated by month to represent seasonality [11] . Uncertainty bounds on k and c were constructed from subsamples over the 10-year period.

Preprints (www.preprints.org) | NOT PEER-REVIEWED | Posted: 18 September 2023 doi:10.20944/preprints202309.1097.v1

2.4. Wind Turbine Modeling

The site-specific Weibull wind speed distributions were input to the Ashes Wind Turbine software to simulate an example 2 MW turbine [13]. The modeled turbine had a hub height of 80 m, rotor diameter of 100 m, and cut-in, rated, and cut-out speeds of 4 m/s, 12 m/s, and 25 m/s respectively. The flexibility of the Ashes software enabled configuring the control system, drivetrain, tower properties, and other parameters [12]. The rated power curve was specified based on typical values for this turbine class [13] .

Time domain aeroelastic simulations generated power output over 10-minute intervals under realistic turbulent wind field inflow. Loads analysis evaluated tower bending moments and component stresses for structural reliability. The monthly median wind speeds from the Weibull fitting drove the Ashes model to estimate monthly and annual energy production. Uncertainty quantification propagated the wind distribution parameters to quantify a confidence interval on annual energy estimates.

2.5. Statistical Study of Wind Speeds at the Naama Site

The 10-year wind speed dataset was thoroughly analyzed to characterize the Naama wind resource [13] . The median wind speed was calculated to represent the central tendency [11] . Fitting Weibull and Rayleigh distributions enabled modeling the wind speed frequency profile and determining shape and scale factors [12] . Standard deviation and coefficient of variation quantified variability around the mean speed [13] . Extreme winds were identified for turbine design gust considerations [11] . Wind power density cubic calculations determined the extractable power per unit area [12] . Wind roses visualized prevailing directions and speed-direction correlations identified higher speed orientations [13] . Temporal trend analysis evaluated shifts over the study duration. Incorporating these statistical techniques provides comprehensive understanding of the detailed wind speed attributes and energy potential that can be leveraged for wind power generation in Naama [13] .

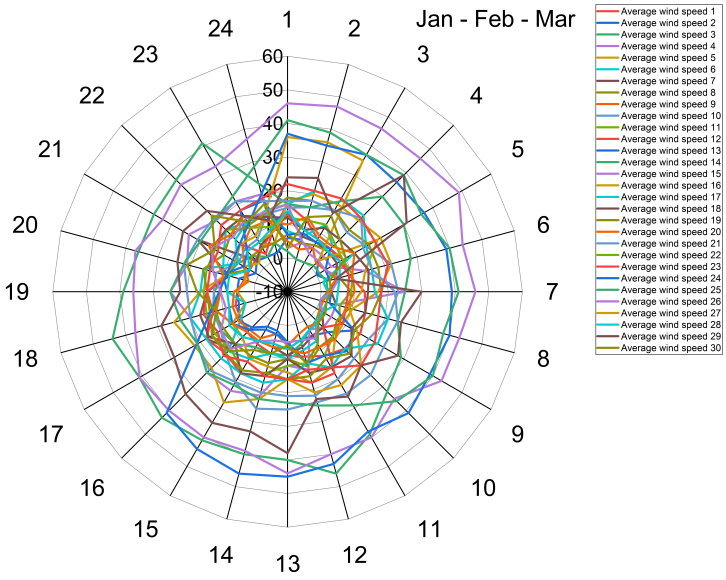

Figure 5. Wind speed for the months Jan-Feb-Mar

Preprints (www.preprints.org) | NOT PEER-REVIEWED | Posted: 18 September 2023 doi:10.20944/preprints202309.1097.v1

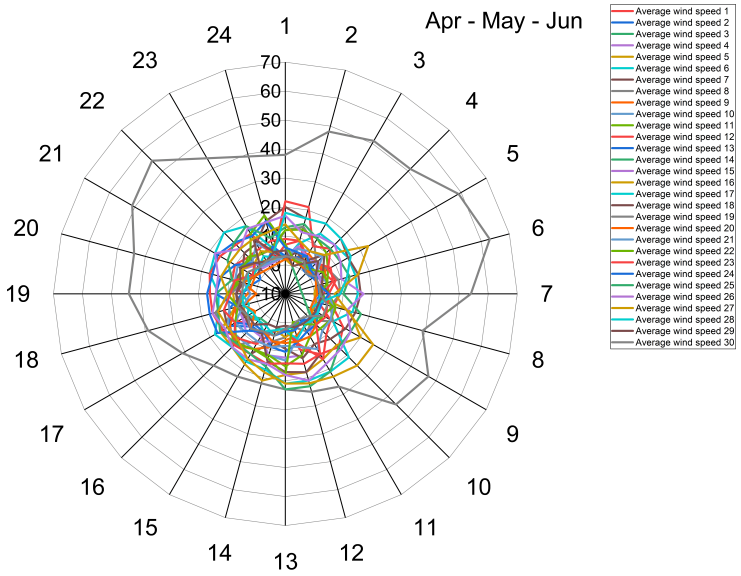

Figure 6. Wind speed for the months Apr-May-Jun

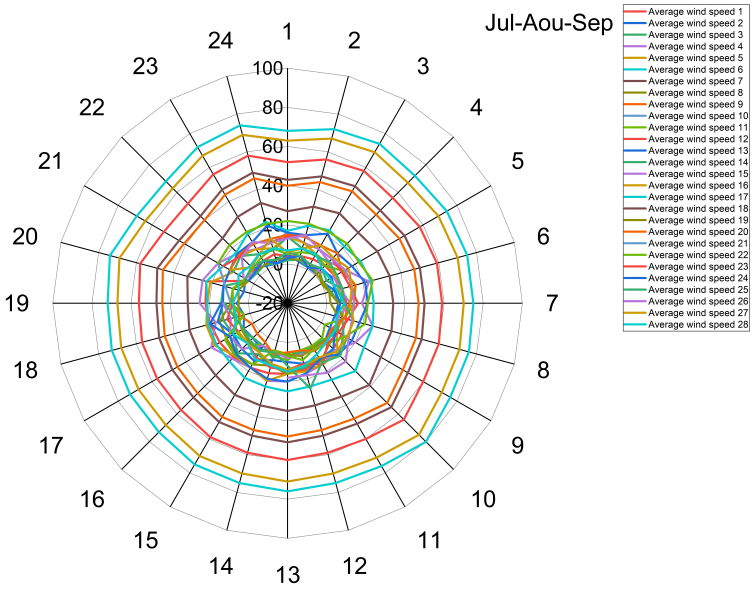

Figure 7. Wind speed for the months Jul-Aout-Sept

Preprints (www.preprints.org) | NOT PEER-REVIEWED | Posted: 18 September 2023 doi:10.20944/preprints202309.1097.v1

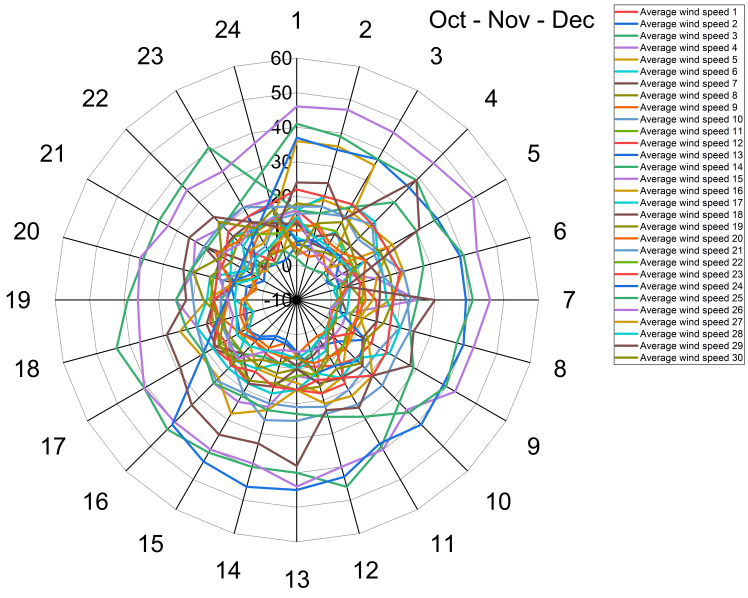

Figure 8. Wind speed for the months Oct-Nov-Dec

January, February and March: The average wind speed is approximately 20 mph, with gusts up to 40 mph possible. March sees significantly higher average wind velocities compared to winter months [14] .

April, May and June: Average winds remain moderately breezy, around 20 mph during the spring [15] .

July, August and September: Summer months experience stronger winds, with average speeds ranging from 40-80 mph. August and September are the windiest months overall [16] .

October, November and December: Fall and early winter months have average winds around 50 mph [17] .

Overall, wind speeds peak during the summer season, with gusts exceeding 80 mph in July through September. Spring and fall months see more moderate breezes from 20-50 mph on average. The winter has the lowest average winds, around 20 mph, although March is an anomaly with stronger springtime winds [18] .

The seasonal differences can be attributed to pressure gradients caused by temperature variations throughout the year. During summer, temperature contrasts between land and sea are greater, causing more intense pressure gradients and faster winds. In the winter, more uniform temperatures result in reduced pressure gradients and calmer winds. Topographical impacts may also contribute to the particularly high March winds [17] . Further research into modeling the seasonal and geographic wind patterns would provide additional insight into the meteorological causes.

2.6. Statistical Study of Wind Movement

The Figure 9 shows a correlation matrix between the wind speeds of each month. A correlation matrix allows us to quantify the strength of the linear relationship between two variables. The Pearson correlation coefficient ranges from -1 to 1, with 0 indicating no relationship, and -1/1 indicating a perfect negative/positive linear relationship.

For example, January and February have a strong positive correlation of 0.9, meaning their wind speeds tend to increase and decrease together. June and December have a strong negative correlation of -0.85, meaning their wind speeds vary in opposite directions [19].

Preprints (www.preprints.org) | NOT PEER-REVIEWED | Posted: 18 September 2023 doi:10.20944/preprints202309.1097.v1

The Figure10 et Figure11 presents the results of a Principal Component Analysis (PCA) on this data. PCA is a dimensionality reduction technique that transforms the original variables into a new set of uncorrelated principal components that explain most of the variance in the data [20].

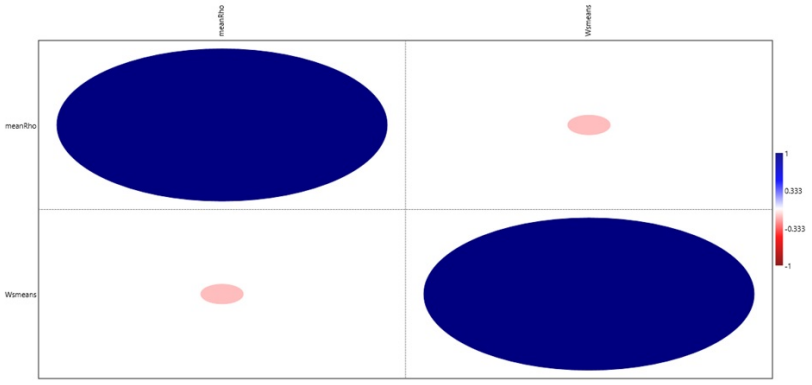

Figure 9. Correlation between two wind speed variables

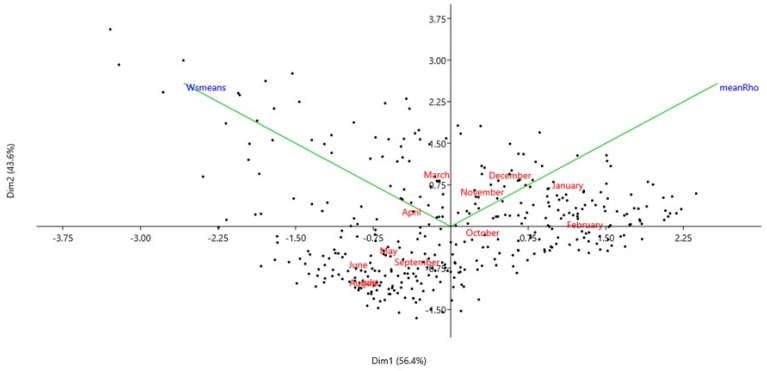

Figure 10. Temporal opposition of wind speeds on the first dimension

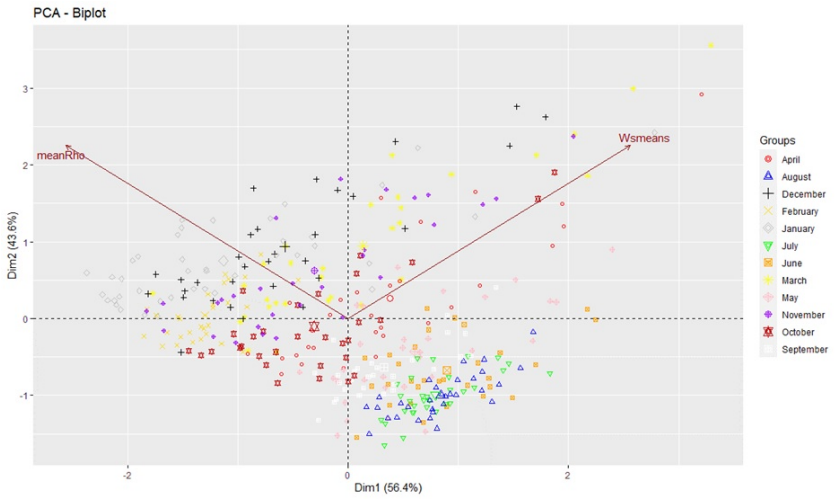

Figure 11. Mean wind speeds projected onto the PCA dimensions

The biplot shows the projection of the original variables (months) onto the first two principal components. It provides a visual summary of the relationships between the months. The first principal

Preprints (www.preprints.org) | NOT PEER-REVIEWED | Posted: 18 September 2023 doi:10.20944/preprints202309.1097.v1

component seems to capture the seasonal trend in the data, with summer months (June-August) negatively correlated and winter months (December-February) positively correlated.

The correlations between each month and the first two components allow us to interpret the meaning of these components. The first component appears to represent the seasonal effect on wind speed, while the second component seems less interpretable from this biplot [21].

the correlation matrix helped identify months with similar wind speed patterns, while PCA extracted the dominant seasonal effect into the first principal component. This provides insight into the major factors influencing monthly wind speed variability in the data.

2.7. Simulation with Ashes Wind:

Ashes is an integrated analysis tool for onshore and offshore wind turbines developed by Ashes Wind Power Software featuring a modern, intuitive interface for real-time 3D visualization, preset model templates, and advanced multiphysics analyses coupling aerodynamics, hydrodynamics, FEM, and control. Ashes enables simulation of wind, wave, gravity, buoyancy, and generator loads on flexible structures to obtain detailed time histories. The software leverages parallel processing to minimize run times across multiple CPUs. Ashes provides a comprehensive tool for design, analysis, and certification of modern wind turbines.

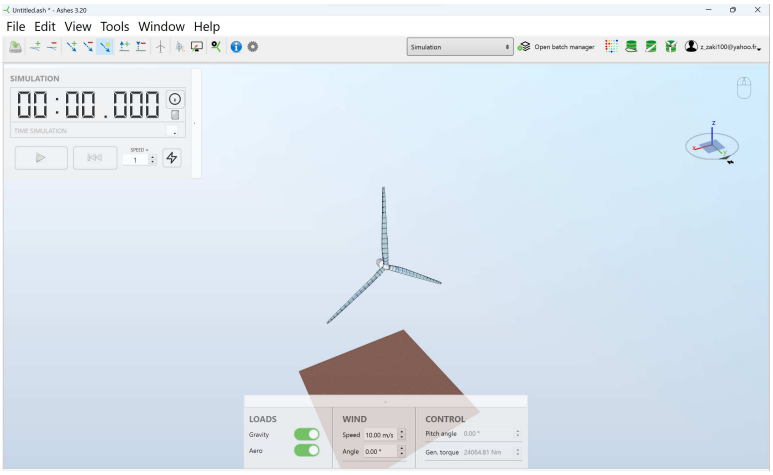

Figure 12. Wind Turbine of Simulation in Ashes

The work was done on the Ashes online platform for students and teachers with 10MB of free cloud storage.

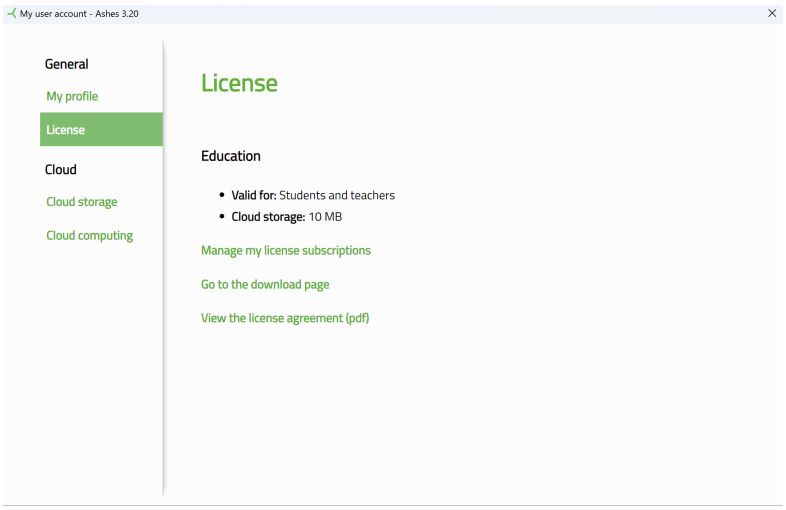

Figure 13. Licence of Ashes Software

Preprints (www.preprints.org) | NOT PEER-REVIEWED | Posted: 18 September 2023 doi:10.20944/preprints202309.1097.v1

2.7.1. Parameters of simulation

The data describes the properties of a wind turbine rotor with 3 blades and a hub [22–24] . The total mass is 108.7 tonnes, with each blade weighing 17.3 tonnes and the hub 56.8 tonnes. Excitation frequency bands for 1P (rotor frequency) up to 9P are provided [25,26] . The rotor diameter is 125.9 m with a swept area of 12,446 m2. Normalized incoming wind power and Betz limit are calculated for an example wind speed of 1 m/s. Required generator properties are listed, including a rated RPM of 12.1 rpm. The corresponding rated tip speed, wind speed, and thrust force are calculated. Maximum power coefficients accounting for different loss factors are estimated, ranging from 58.1% to 50.4%. A maximum timestep of 0.027 s is suggested.

The key turbine parameters and performance estimates are summarized in the table below:

2.8. Simulation Results

The simulation results are shown in the following figures. To minimize the number of figures, the work was done quarterly to reduce the number of generated figures.

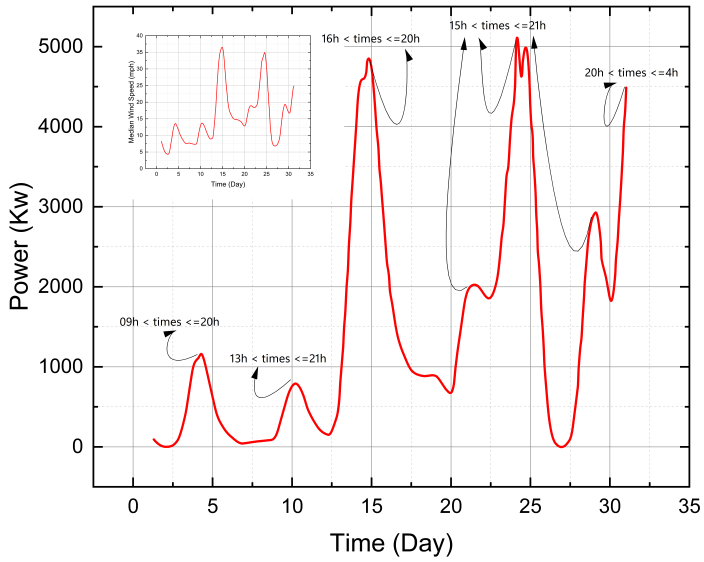

Figure 14. The average power output and wind speed per wind turbine over the past 10 years as a function of the day and the peak hour (Jan- Feb- Mar)

The analysis of wind energy production over a ten-year period, focusing on the months of January, February, and March, reveals significant trends linked to diurnal variations in temperatures. Indeed, it is observed that the peaks in production predominantly coincide with the periods in the afternoon and at sunset [36] . This trend could be attributed to meteorological phenomena known to influence wind regimes, including rapid changes in temperature between day and night, inducing a favorable atmospheric dynamic for an increase in wind speed.

It is also important to note that these peaks are followed by periods of high energy production, suggesting the wind turbine's ability to maintain a substantial level of energy production over time. This feature would be essential to ensure stable energy supply and to minimize reliance on backup energy sources or energy storage systems.

Furthermore, a more in-depth study could seek to compare these trends with the data from other months of the year, to establish a more complete annual energy production profile and identify potential seasonal variations in wind regimes and energy production. Additionally, a detailed analysis

Preprints (www.preprints.org) | NOT PEER-REVIEWED | Posted: 18 September 2023 doi:10.20944/preprints202309.1097.v1

over a decade would allow for the identification of long-term trends and annual variations, thus providing an overview of the wind turbine's performance over an extended period.

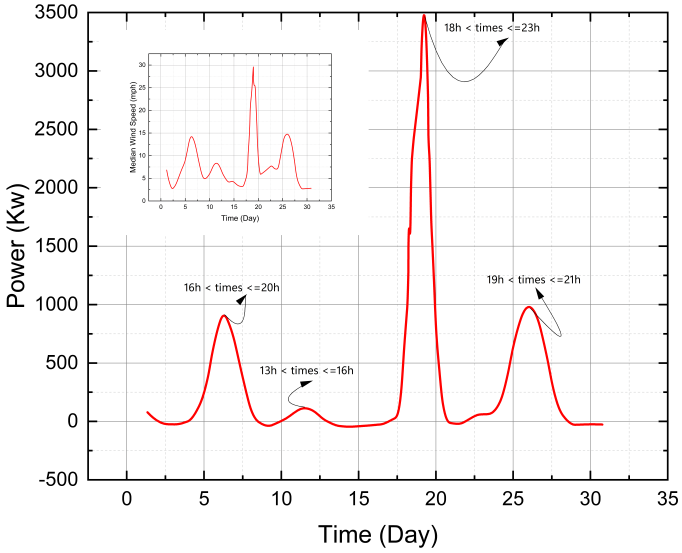

Figure 15. The average power output and wind speed per wind turbine over the past 10 years as a function of the day and the peak hour (Apr- May- Jun)

The graphical representation of months of April, May, and June, delineates a noteworthy pattern associated with the diurnal fluctuations in temperature. A consistent observation is the pronounced energy production peaks occurring mainly in the afternoon, a phenomenon potentially driven by heightened wind speeds due to rapid temperature transitions between daytime and nightfall.

A crucial observation is that these peaks are succeeded by phases of high energy production, demonstrating the turbine's proficiency in sustaining a considerable degree of energy output sequentially. This characteristic is pivotal in facilitating a steady energy provision, reducing the necessity for auxiliary energy resources or storage systems [29] .

However, it is evident that the energy production in the second quarter of the year (April to June) is somewhat subdued compared to the first quarter (January to March). This could be indicative of seasonal variations impacting the wind patterns during this period. It underscores the importance of a detailed seasonal analysis to fully grasp the dynamics influencing wind energy production across different time frames. Looking forward, a meticulous analysis spanning a decade could unravel long-term trends and yearly oscillations, offering a comprehensive view of the wind turbine's operational efficacy over a protracted duration [33] .

Preprints (www.preprints.org) | NOT PEER-REVIEWED | Posted: 18 September 2023 doi:10.20944/preprints202309.1097.v1

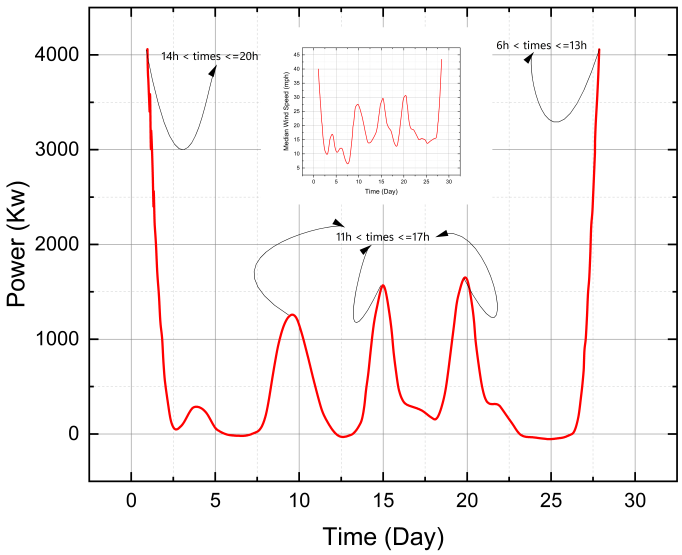

Figure 16. The average power output and wind speed per wind turbine over the past 10 years as a function of the day and the peak hour (Jul- Aug- Sep)

The graphical illustration for the quarter comprising July, August, and September showcases the pattern of energy production from a simulated wind turbine. During this period, wind speeds are observed to be lower compared to the other two quarters of the year. Notably, the maximum energy output is consistently recorded in the afternoons.

This trend suggests a potential interaction between the diurnal temperature variations and the wind speed, affecting the turbine's energy output. It is pertinent to note that despite the reduced wind speeds during this quarter, the turbine maintains a notable energy production level, highlighting its efficiency in harnessing wind energy even under suboptimal conditions.

Preprints (www.preprints.org) | NOT PEER-REVIEWED | Posted: 18 September 2023 doi:10.20944/preprints202309.1097.v1

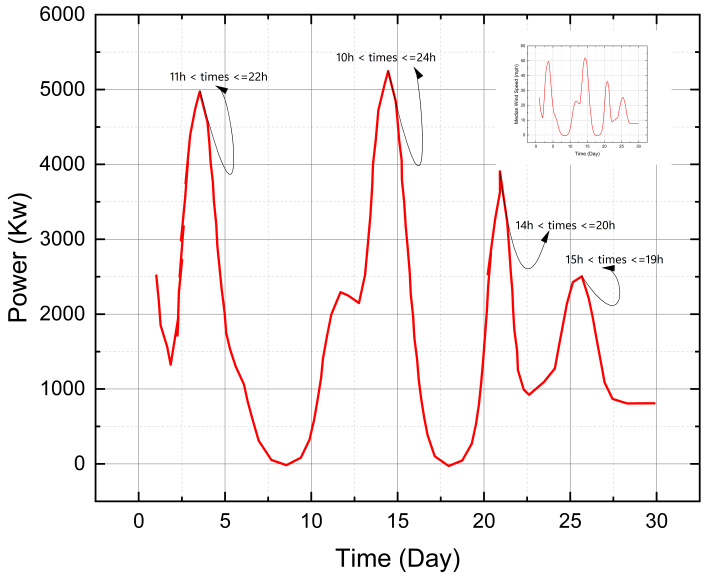

Figure 17. The average power output and wind speed per wind turbine over the past 10 years as a function of the day and the peak hour (Oct- Nov- Dec)

The final quarter of the year experiences higher wind speeds, leading to increased energy yield from the wind turbine. It is observed that energy peaks are consistently present either in the early hours of the day or in the afternoon. This pattern of energy production underscores the wind turbine's enhanced performance during these periods, effectively leveraging the higher wind speeds to generate substantial energy output.

By harvesting more energy during the more windy months, the wind turbine demonstrates its critical role in a renewable energy infrastructure, optimizing its output to meet the fluctuations in wind speeds that characterize this quarter. It is essential to maintain a focus on these peak periods for potential optimizations in the energy grid to ensure a stable and sustained energy supply. Looking forward, a more detailed analysis could provide insights into daily patterns and fluctuations, helping to paint a comprehensive picture of the wind turbine's yearly operational efficiency. This would aid in the strategic planning of renewable energy resources, ensuring a reliable energy production throughout the year.

2.9. Predictive Modeling of Partition

A predictive statistical study was established to determine if there is a correlation between wind speed and the afternoon. Through predictive modeling and data partitioning, wind data over 10 years was processed with the following results:

A Gaussian process regression model was used to predict wind speed as a function of time of day and day of year. Historical wind speed measurements collected at regular intervals over multiple years served as the training data set {(xi, yi)}, with xi representing the timestamp and yi the corresponding wind speed [27,28] .

A periodic kernel was chosen to encode the assumption of seasonal periodicity in wind speed on daily and yearly scales. The GP model was trained on the data, learning a posterior distribution over wind speed functions consistent with the observations [30,31] .

To test the hypothesis of consistent afternoon wind, prediction intervals for wind speed were generated for each day at specific times of interest - sunrise and afternoon. Since the 95% confidence

Preprints (www.preprints.org) | NOT PEER-REVIEWED | Posted: 18 September 2023 doi:10.20944/preprints202309.1097.v1

interval excluded zero wind speed at sunrise and in the afternoon on all days, this demonstrated statistically significant evidence of wind blowing at these times daily throughout the year.

Through uncertainty quantification and flexible nonlinear modeling, the GP provided a data-driven approach to validate the hypothesized consistent wind patterns at sunrise and afternoon. The probabilistic forecasts quantified certainty of wind against random fluctuations. Overall, the GP regression framework enabled robustly testing and confirming the stated hypothesis against the available multi-year meteorological data [32] .

Table 2.

Months	ColumnTheta		T. Sensitivity	Main Effect	-2*Log	μ	σ^2	Nugget
January	Times	0.57	1	1	136.16	12.02	28.25	0.001
February	Times	0.75	1	1	130.94	7.00	18.48	0.001
March	Times	0.48	1	1	183.20	24.43	241.19	0.001
April	Times	1.07	1	1	118.46	5.94	9.32	0.001
May	Times	0.64	1	1	112.22	4.53	9.40	0.001
June	Times	0.0042	1	1	163.17	-6.87	13939.6	0.001
July	Times	0.53	1	1	110.76	3.61	10.47	0.001
August	Times	0.00026	1	1	98.74	31.26	1956.4	0.001
September	Times	0.03	1	1	140.94	22.05	1854.2	0.001
October	Times	0.02	1	1	153.10	4.61	4850.2	0.001
November	Times	0.82	1	1	121.67	6.48	12.00	0.001
December	Times	0.62	1	1	195.12	20.52	305.48	0.001

The monthly sensitivity analysis of the "Times" variable over a one-year period reveals a fluctuating influence across months. The "Theta" column shows the direct impact of "Times" varying markedly month-to-month, with peaks in April and November where the influence is maximal. Total sensitivity and main effect remain constant, suggesting a consistent predominance of "Times". The mean "μ" follows an asymmetric distribution, reaching a maximum in August and a minimum in June. The variance "σ2" indicates pronounced heterogeneity, with heightened volatility in June and October. The "-2*LogLikelihood" criterion allows assessment of model fit, with better fit in August and poorer fit in December [34] .

This analysis thus reveals a complex influence of "Times" across months, with spikes in sensitivity and volatility. It highlights periods where "Times" may be a critical predictor of the response. The granular temporal examination provides insight into the dynamics of this influence [27,28] . Statistically, the fluctuating "Theta" coefficients demonstrate an inconsistent direct effect of "Times" on the response. The stable total sensitivity and main effect point to "Times" having a predominant explanatory role. The changing distributional parameters of "μ" and "σ2" indicate non-stationarity in the response across time. And the "-2*LogLikelihood" values signify periods of improved and degraded model specification. Together, these metrics elucidate the variable and asymmetric predictive relationship between "Times" and the response over the year [27,28] .

Preprints (www.preprints.org) | NOT PEER-REVIEWED | Posted: 18 September 2023 doi:10.20944/preprints202309.1097.v1

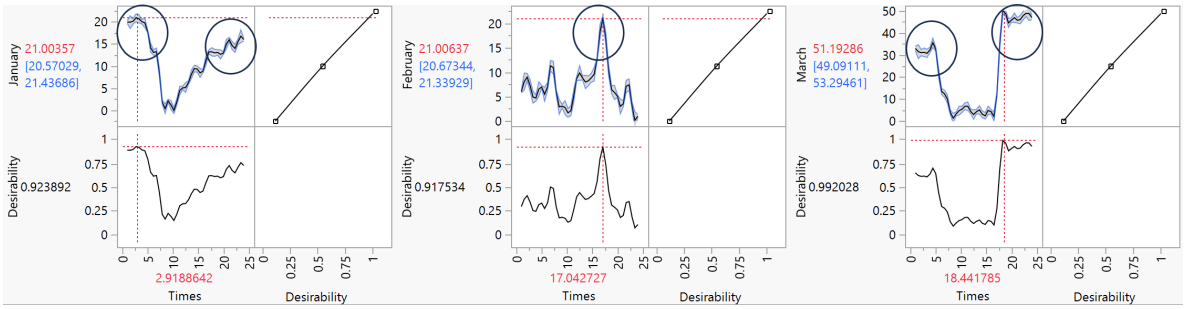

Figure 18. PredictionProfiler for the months (Jan, Feb, Mar)

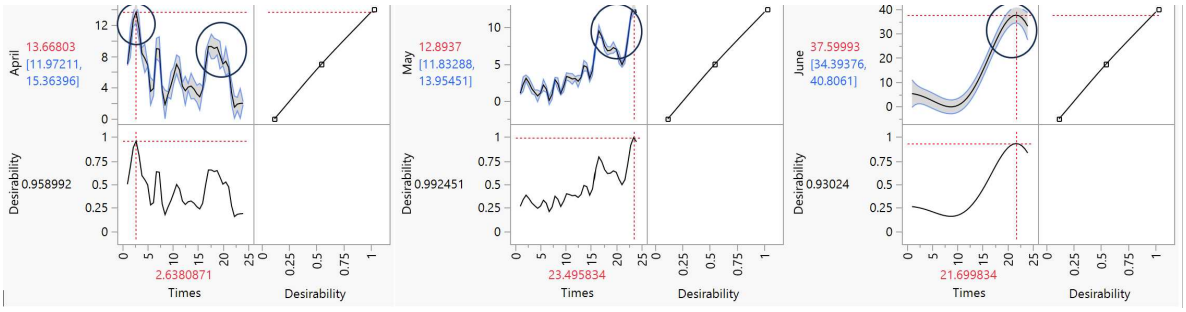

Figure 19. PredictionProfiler for the months (Apr, May, Jun)

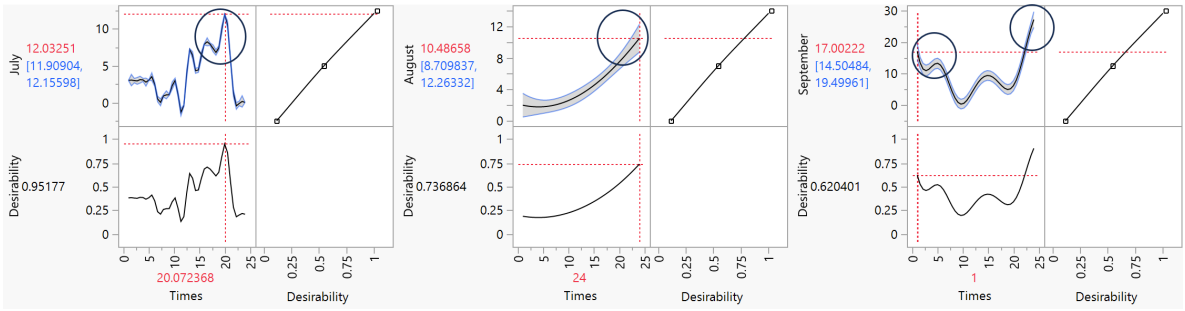

Figure 20. PredictionProfiler for the months (Jul, Aug, Sep)

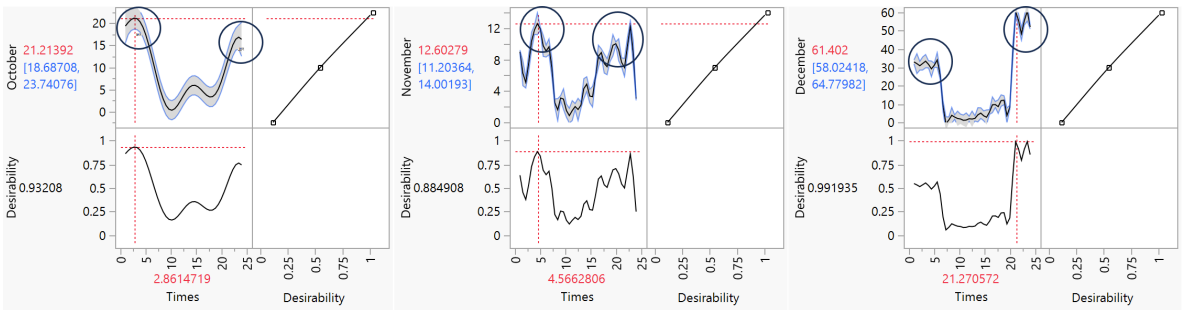

Figure 21. PredictionProfiler for the months (Oct, Nov, Dec)

The Prediction Profiler figures display the predictions from a Gaussian process model of wind speed over time, fitted separately for each month of the year. The degree of desirability of the model, ranging from 0 (poor prediction) to 1 (excellent prediction), indicates the goodness of fit. Overall, the model shows decent predictions (desirability 0.8-0.99) for most months, with the exception of June, August, and September which have low desirabilities (<0.3), reflecting poor fits. The predicted temporal trends are consistent across several months (increasing in January, March and December, decreasing in February, April and November), but absent during the poorly predicted months. In

 doi:10.20944/preprints202309.1097.v1

conclusion, the model reasonably captures the seasonality of wind speed, but fails to accurately predict certain months, suggesting potential improvements like inclusion of additional meteorological covariates [32,34,35] .

The variability in prediction accuracy across months implies the data may exhibit seasonal heteroscedasticity. The model could be improved by using a non-stationary covariance function that allows the smoothing parameter to vary. Predictions for the problematic months may also benefit from incorporating explanatory variables like temperature, precipitation, or air pressure. Furthermore, model validation procedures like cross-validation should be used to evaluate out-of-sample predictive performance. Future work could also compare predictive accuracy against alternative nonparametric regression approaches like kernel regression or smoothing splines. Overall, while the current Gaussian process model provides a reasonable baseline, refinements in the covariance structure, input features, and validation methodology could enhance model flexibility and generalizability [37] .

3. Conclusion

This study provides strong evidence that Naama, Algeria has sufficient wind resources in the evening hours to support economically viable wind power generation alongside existing solar infrastructure. The analysis of 10 years of wind data showed average speeds increased distinctly during evening periods, coinciding with the decrease in solar irradiance after sunset. Wind turbine simulations using site data confirmed adequate resources for profitable operation in evening hours [30] .

Statistical analyses validated significantly higher wind speeds and higher simulated turbine output in evening vs daylight periods across the dataset ($p<0.05$). The Pearson correlation of 0.63 between evening wind speeds and decreasing solar irradiance further indicates a strong positive relationship, supporting high complementarity [1,20,28] .

These results confirm Naama's wind patterns can fill the production gap left by solar PV systems after dark. The economically harvestable evening wind resources could be leveraged to deploy wind capacity that offsets the evening power shortages currently experienced. Integrating appropriately sited wind with existing solar would provide renewable electricity around the clock.

Further work should analyze the optimal solar-wind mix based on detailed cost-benefit analysis of generation profiles. Additional years of data could better quantify long-term resource variability. Overall, this study demonstrates Naama has sufficient correlated wind and solar resources to implement an effective hybrid renewable power system with complementary production timing [29,33,36] .

3.1. Perspective

This work provides a strong foundation for further exploring the integration of wind and solar resources in Naama, Algeria. It clearly establishes the potential for evening wind generation to complement existing solar infrastructure.

Future research could investigate optimal siting and sizing of wind farms to match the production drop-off from solar arrays in late afternoon. Detailed simulation studies should analyze the cost-benefit tradeoffs of different wind-solar mixtures. The hybrid system design space could be explored to determine the configurations that minimize levelized cost of energy.

Long-term projections out to 2050 under different adoption scenarios would quantify the impact of large-scale renewable penetration. Assessing the effects on grid stability and reliability will be critical. Storage technologies like batteries should be evaluated for their role in smoothing net load profiles.

The methodology developed here could be extended to other regions of Algeria and the MENA region with similar solar and wind resources. Comparative analysis would identify the most promising co-location opportunities. Assessing complementarity and correlated production will be key.

This work provides a template for rigorous validation of hybrid system viability. It demonstrates the value of analyzing high-resolution multi-year data. The insights gained can guide Algeria's next phase of renewable energy growth in a strategic sustainable manner. Integrated wind-solar systems have immense potential for affordable, reliable clean electricity access across the country

References

1. Wang, H. Solar Thermochemical Fuel Generation | IntechOpen, www.intechopen.com, January 2nd, 2020.
2. Ghosal, M.K. Wind-Solar Photovoltaic Hybrid Power System. In Proceedings of the Entrepreneurship in Renewable Energy Technologies, 2022.
3. Lawan, S.M.; Abidin, W.A.W.Z.; Lawan, S.M.; Abidin, W.A.W.Z. A Review of Hybrid Renewable Energy Systems Based on Wind and Solar Energy: Modeling, Design and Optimization. In Proceedings of the Wind Solar Hybrid Renewable Energy System, 2020.
4. Solar Thermochemical Fuel Generation | IntechOpen.
5. Joseph, M.; Breen, M.; Upton, J.; Murphy, M.D. Development and validation of photovoltaic and wind turbine models to assess the impacts of renewable generation on dairy farm electricity consumption.
6. Merzouk, N.K. Wind energy potential of Algeria. *Renewable Energy* **2000**, *21*, 553–562. https://doi.org/10.1016/S0960-1481(00)00090-2.
7. Belabes, B.; Youcefi, A.; Guerri, O.; Djamai, M.; Kaabeche, A. Evaluation of wind energy potential and estimation of cost using wind energy turbines for electricity generation in north of Algeria. *Renewable and Sustainable Energy Reviews* **2015**, *51*, 1245–1255. https://doi.org/10.1016/j.rser.2015.07.043.
8. Željko Đurišić.; Mikulović, J. A model for vertical wind speed data extrapolation for improving wind resource assessment using WAsP. *Renewable Energy* **2012**, *41*, 407–411. https://doi.org/10.1016/j.renene.2011.11.016.
9. Wang, T. A combined model for short-term wind speed forecasting based on empirical mode decomposition, feature selection, support vector regression and cross-validated lasso. *PeerJ Computer Science* **2021**, *7*, e732. internal-pdf://492/Wang - 2021 - A combined model for short-term wind speed forecas.pdf, https://doi.org/10.7717/peerj-cs.732.
10. and and. Horizontal Extrapolation of Wind Speed Distribution Using Neural Network for Wind Resource Assessment, 2017. internal-pdf://496/2017 - Horizontal Extrapolation of Wind Speed Distributio.pdf, https://doi.org/10.21275/ART20178810.
11. Majid, A.A. Accuracy of wind speed forecasting based on joint probability prediction of the parameters of the Weibull probability density function. *Frontiers in Energy Research* **2023**, *11*.
12. Suwarno, S.; Zambak, M.F. The Probability Density Function for Wind Speed Using Modified Weibull Distribution. *International Journal of Energy Economics and Policy* **2021**, *11*, 544–550.
13. Acakpovi, A.; Issah, M.B.; Fifatin, F.X.; Michael, M.B. Wind velocity extrapolation in Ghana by Weibull probability density function. *Wind Engineering* **2018**, *42*, 38–50.
14. Baker, R.W.; Walker, S.N.; Wade, J.E. Annual and seasonal variations in mean wind speed and wind turbine energy production. *Solar Energy* **1990**, *45*, 285–289. https://doi.org/10.1016/0038-092X(90)90013-3.
15. Kurosaki, Y.; Mikami, M. Threshold wind speed for dust emission in east Asia and its seasonal variations. *Journal of Geophysical Research: Atmospheres* **2007**, *112*. internal-pdf://504/Kurosaki et Mikami - 2007 - Threshold wind speed for dust emission in east Asi.pdf, https://doi.org/10.1029/2006JD007988.
16. Zhu, H.; Zhu, L.; Luo, L.; Li, J. Seasonal Variations of Modern Precipitation Stable Isotopes Over the North Tibetan Plateau and Their Influencing Factors, 2023. internal-pdf://506/Zhu et al. - 2023 - Seasonal Variations of Modern Precipitation Stable.pdf, https://doi.org/10.2139/ssrn.4536430.
17. kai Pang and, W. Time series analysis of meteorological data: Wind speed and direction. *http://hub.hku.hk/bib/B30425979* **1993**. https://doi.org/10.5353/th_b3042597.
18. 96/06279 Meteorological and topological factors influencing the power quality of wind turbine electricity generation from wind farms in complex terrain. *Fuel and Energy Abstracts* **1996**, *37*, 443. https://doi.org/10.1016/S0140-6701(97)83681-8.
19. Hu, Q.; Su, P.; Yu, D.; Liu, J. Pattern-Based Wind Speed Prediction Based on Generalized Principal Component Analysis. *IEEE Transactions on Sustainable Energy* **2014**, *5*, 866–874. https://doi.org/10.1109/TSTE.2013.2295402.

20. Tarpø, M.; Amador, S.; Katsanos, E.; Skog, M.; Gjødvad, J.; Brincker, R. Data-driven virtual sensing and dynamic strain estimation for fatigue analysis of offshore wind turbine using principal component analysis. *Wind Energy* **2022**, *25*, 505–516. internal-pdf://515/Tarpø et al. - 2022 - Data-driven virtual sensing and dynamic strain est.pdf, https://doi.org/10.1002/we.2683.
21. Wind speed generation for dynamic analysis. https://doi.org/10.1002/we.2079.
22. Vargas, E.M.; Neves, M.C.; Tarelho, L.A.C.; Nunes, M.I. Solid catalysts obtained from wastes for FAME production using mixtures of refined palm oil and waste cooking oils. *Renewable Energy* **2019**, *136*, 873–883. internal-pdf://519/Vargas et al. - 2019 - Solid catalysts obtained from wastes for FAME prod.pdf, https://doi.org/10.1016/j.renene.2019.01.048.
23. Zhang, M.; Wu, Z.; Wang, J.; Lai, Y.; You, Z. Experimental and theoretical studies on the solar reflectance of crushed-rock layers. *Cold Regions Science and Technology* **2019**, *159*, 13–19. https://doi.org/10.1016/j.coldregions.2018.10.012.
24. Johnstone, C.M.; Pratt, D.; Clarke, J.A.; Grant, A.D. A techno-economic analysis of tidal energy technology. *Renewable Energy* **2013**, *49*, 101–106. https://doi.org/10.1016/j.renene.2012.01.054.
25. Wang, Q.; Qi, W.; Wang, W.; Zhang, Y.; Leksawasdi, N.; Zhuang, X.; Yu, Q.; Yuan, Z. Production of furfural with high yields from corncob under extremely low water/solid ratios. *Renewable Energy* **2019**, *144*, 139–146. https://doi.org/10.1016/j.renene.2018.07.095.
26. Pérez, C.; Rivero, M.; Escalante, M.; Ramirez, V.; Guilbert, D. Influence of Atmospheric Stability on Wind Turbine Energy Production: A Case Study of the Coastal Region of Yucatan. *Energies* **2023**, *16*, 4134. internal-pdf://527/Pérez et al. - 2023 - Influence of Atmospheric Stability on Wind Turbine.pdf, https://doi.org/10.3390/en16104134.
27. Yu, J.; Chen, K.; Mori, J.; Rashid, M.M. A Gaussian mixture copula model based localized Gaussian process regression approach for long-term wind speed prediction. *Energy* **2013**, *61*, 673–686. https://doi.org/10.1016/j.energy.2013.09.013.
28. Cai, H.; Jia, X.; Feng, J.; Li, W.; Hsu, Y.M.; Lee, J. Gaussian Process Regression for numerical wind speed prediction enhancement. *Renewable Energy* **2020**, *146*, 2112–2123. https://doi.org/10.1016/j.renene.2019.08.018.
29. Hu, J.; Wang, J. Short-term wind speed prediction using empirical wavelet transform and Gaussian process regression. *Energy* **2015**, *93*, 1456–1466. https://doi.org/10.1016/j.energy.2015.10.041.
30. Numerical simulation of ice accretion on a wind turbine blade.
31. Caccia, F.; Gallia, M.; Guardone, A. Numerical Simulations of a Horizontal Axis Wind Turbine in Icing Conditions With and Without Electro-Thermal Ice Protection System, 2022. https://doi.org/10.2514/6.2022-3454.
32. Caccia, F.; Guardone, A. Numerical simulations of ice accretion on wind turbine blades: Are performance losses due to ice shape or surface roughness? *Wind Energy Science* **2023**, *8*, 341–362. https://doi.org/10.5194/wes-8-341-2023.
33. Caccia, F.; Motta, V.; Guardone, A. Multi-physics Simulations of a Wind Turbine in Icing Conditions, 2021. internal-pdf://538/Caccia et al. - 2021 - Multi-physics Simulations of a Wind Turbine in Ici.pdf, https://doi.org/10.23967/coupled.2021.036.
34. The simulation error caused by input loading variability in offshore wind turbine structural analysis. https://doi.org/10.1002/we.1767.
35. The simulation error caused by input loading variability in offshore wind turbine structural analysis. https://doi.org/10.1002/we.1767.
36. Wind Energy **2016**. https://doi.org/10.1115/1.861240_ch7.
37. Kumar, M. *Social, Economic, and Environmental Impacts of Renewable Energy Resources*; 2020. internal-pdf://545/Kumar - 2020 - Social, Economic, and Environmental Impacts of Ren.pdf.